

# Depletion of phosphatidylcholine affects endoplasmic reticulum morphology and protein traffic at the Golgi complex

Nicole Testerink, Michiel H. M. van der Sanden, Martin Houweling, J. Bernd Helms, and Arie B. Vaandrager<sup>1</sup>

Department of Biochemistry and Cell Biology, Faculty of Veterinary Medicine, and Institute of Biomembranes, University of Utrecht, 3584 CM, The Netherlands

**Abstract** The mutant Chinese hamster ovary cell line MT58 contains a thermosensitive mutation in CTP:phosphocholine cytidyltransferase, the regulatory enzyme in the CDP-choline pathway. As a result, MT58 cells have a 50% decrease in their phosphatidylcholine (PC) level within 24 h when cultured at the nonpermissive temperature (40°C). This is due to a relative rapid breakdown of PC that is not compensated for by the inhibition of de novo PC synthesis. Despite this drastic decrease in cellular PC content, cells are viable and can proliferate by addition of lysophosphatidylcholine. By [<sup>3</sup>H]oleate labeling, we found that the FA moiety of the degraded PC is recovered in triacylglycerol. In accordance with this finding, an accumulation of lipid droplets is seen in MT58 cells. Analysis of PC-depleted MT58 cells by electron and fluorescence microscopy revealed a partial dilation of the rough endoplasmic reticulum, resulting in spherical structures on both sites of the nucleus, whereas the morphology of the plasma membrane, mitochondria, and Golgi complex was unaffected. In contrast to these morphological observations, protein transport from the ER remains intact. Surprisingly, protein transport at the level of the Golgi complex is impaired. Our data suggest that the transport processes at the Golgi complex are regulated by distal changes in lipid metabolism.—Testerink, N., M. H. M. van der Sanden, M. Houweling, J. B. Helms, and A. B. Vaandrager. Depletion of phosphatidylcholine affects endoplasmic reticulum morphology and protein traffic at the Golgi complex. *J. Lipid Res.* 2009. 50: 2182–2192.

**Supplementary key words** CTP:phosphocholine cytidyltransferase • lipid droplets • protein transport • diacylglycerol

Phosphatidylcholine (PC) is the major phospholipid species in eukaryotic cell membranes, generally comprising ~50% of the total phospholipid mass of most cells and their organelles. In mammalian cells, PC is mainly synthesized de novo via the CDP-choline pathway (1). The major

ity of PC produced by the CDP-choline pathway is used for membrane assembly as PC or as a precursor for other membrane phospholipids like phosphatidylserine and sphingomyelin (1). In addition to its structural role, PC also functions as a major source of intracellular signaling molecules (2–4). Agonist-stimulated hydrolysis of PC by either phospholipase C or the combined action of phospholipase D and phosphatidate phosphohydrolase results in an elevation of diacylglycerol (DAG) levels in the cell (2). DAG is an activator of the protein kinase C family of enzymes involved in biological processes, such as proliferation and differentiation (5). It has therefore been suggested that PC synthesis is tightly regulated in accordance with requirements for membrane turnover and cell proliferation (6).

The enzyme CTP:phosphocholine cytidyltransferase (CT) catalyzes a major regulatory step in the CDP-choline pathway (1). This enzyme is primarily localized to the nucleus, cytosol, and endoplasmic reticulum (ER) (7, 8). CT activity in cells is controlled by association with membrane lipids and by gene expression (9–11). Inhibition of CT by pharmacological drugs like hexadecylphosphocholine leads to the inhibition of cell growth and increased apoptosis (12). Furthermore, a Chinese hamster ovary (CHO) cell line, MT58, which contains a thermosensitive, inhibitory mutation in CT $\alpha$ , has been established and was shown to have severely reduced levels of PC at the nonpermissive temperature, resulting in growth inhibition and eventu-

Abbreviations: CHO, Chinese hamster ovary; CT, CTP:phosphocholine cytidyltransferase; DAG, diacylglycerol; EM, electron microscopy; ER, endoplasmic reticulum; FRAP, fluorescence recovery after photobleaching; LD, lipid droplet; lysoPC, lysophosphatidylcholine; PC, phosphatidylcholine; PKD, protein kinase D; pVSVG-GFP, plasmid containing the coding sequence for vesicular stomatitis virus glycoprotein fused to green fluorescent protein; RLU, relative light units; TAG, triacylglycerol; TGN, trans-Golgi network; YFP, yellow fluorescent protein.

<sup>1</sup>To whom correspondence should be addressed.  
e-mail: a.b.vaandrager@uu.nl

Manuscript received 19 December 2008 and in revised form 24 April 2009 and in re-revised form 19 May 2009.

Published, JLR Papers in Press, May 20, 2009  
DOI 10.1194/jlr.M800660-JLR200

Copyright © 2009 by the American Society for Biochemistry and Molecular Biology, Inc.

ally, after 48 h, in an increase in apoptosis (13–18). In a previous study, we showed that shifting MT58 cells to the nonpermissive temperature of 40°C leads to an inhibition in PC synthesis within 5 h and a subsequent rapid depletion of the amount of PC (>50%) within 24 h (17). At this time point, the PC-depleted MT58 cells are still viable and have a comparable CHO-K1 growth rate; addition of lysophosphatidylcholine (lysoPC) around 30 h can rescue them from apoptosis (17).

This study was designed to investigate the effects of inhibition of PC synthesis on PC metabolism and on morphological and functional changes in MT58 cells. Here, we report that inhibition of PC synthesis results in a disturbance of the morphological structure of the ER, accompanied by an impaired protein transport at the Golgi complex. Furthermore, an accumulation of lipid droplets (LDs) is observed, caused by an increase in intracellular triacylglycerol (TAG).

## MATERIALS AND METHODS

### Materials

Ham's F-12 medium, FBS, and calcium-free PBS was purchased from Gibco BRL (Grand Island, NY). [*methyl*-<sup>3</sup>H] Choline chloride (83.0 Ci/mmol), [9,10(*n*)-<sup>3</sup>H] oleic acid (7 Ci/mmol), and [1-<sup>14</sup>C]palmitoyl-CoA (55 mCi/mmol) were obtained from Amersham Pharmacia Biotech (Little Chalfont, UK). Penicillin, streptomycin, trypsin/EDTA solution, and Bodipy 493/503 were from Molecular Probes (Breda, The Netherlands), and all other chemicals were from Sigma-Aldrich (Poole, UK). Mouse monoclonal anti-PDI was purchased from Stressgen (Victoria, BC, Canada), mouse monoclonal anti-GM130 from BD Biosciences (San Jose, CA), rabbit anti-mouse IgG from Dako (Glostrup, Denmark), and PAG10nm from CMC-UMC (Utrecht, The Netherlands). The monoclonal antibody against the extracellular domain of VSVG was a generous gift of Dr. Pepperkok. Prefab Silica Gel G TLC plates were purchased from Merck (Darmstadt, Germany). Coomassie<sup>®</sup> Plus Protein assay reagent kit was supplied by Pierce (Cheshire, UK). All other nonspecified chemicals were of analytical grade.

### Cell culture

Wild-type CHO-K1 and CHO-MT58 (14, 15) cell lines were cultured in Ham's F-12 medium supplemented with 7.5% FBS, 100 units/ml penicillin, and 100 µg/ml streptomycin. MT58 cells stably expressing ER-targeted enhanced yellow fluorescent protein (YFP) were made by transfecting MT58 cells with pEYFP-ER (Clontech Laboratories, Mountain View, CA). All cells were maintained at 33°C, 5% CO<sub>2</sub>, and 90% relative humidity and subcultured twice a week.

### Determination of PC degradation

The PC pool was labeled to equilibrium by incubation of the cells under standard culture conditions at 33°C in 60 mm dishes containing 3 ml of DMEM with 7.5% FBS and 2 µCi (<sup>3</sup>H)choline for 48 h or in Ham's F-12 medium with 7.5% FBS and 1 µCi [<sup>3</sup>H]oleate for 24 h. After removal of the label by three washes with medium, the PC degradation was determined by incubating the cells in 3 ml Ham's F-12 medium (100 µM choline) containing 7.5% FBS for 2 or 22 h at either the permissive temperature (33°C) or the nonpermissive temperature (40°C). Subsequently, the cells were washed with ice-cold PBS, after which 1 ml of meth-

anol and 0.8 ml of water were added. Lipids and water-soluble products were extracted from the cells by the method of Bligh and Dyer (19). Radioactivity in the water phase was measured directly by liquid scintillation counting. The extracted lipids were separated by TLC on prefab silica G plates in a solvent system of chloroform/methanol/water 65:35:4 (v/v/v) in the case of phospholipids and in a solvent system of petroleum ether/diethyl ether 80:20 (v/v) in the case of neutral lipids. [<sup>3</sup>H] containing spots were scraped off, and radioactivity in the spots was measured by liquid scintillation counting.

### Determination of TAG

Cells grown in 60 mm dishes were washed with ice-cold PBS. Lipids were extracted from the cells by the method of Bligh and Dyer (19). Dried lipids were first resuspended in 0.2 ml 10% Triton X-100 in chloroform, and after evaporation of the chloroform, 0.3 ml of water was added. Subsequently, TAG was hydrolyzed by lipase (from *Pseudomonas* sp. Type XIII; 2 units; Sigma-Aldrich), and the released glycerol was determined by coupled enzymatic reactions (20).

### Determination of diacylglycerolacyltransferase activity

Cells grown in 60 mm dishes were washed with ice-cold PBS and scraped into 1 ml of PBS. Cells were homogenized by sonication (2 × 15''), and diacylglycerolacyltransferase (DGAT) activity was determined by adding 50 µl of the homogenate (~50 µg protein) to 250 µl reaction mix finally containing 175 mM Tris-HCl (pH 7.4), 8 mM MgCl<sub>2</sub>, 1 mg/ml BSA, 4 mM DAG in 0.12 mg/ml Tween 20, 30 µM palmitoyl-CoA, and 0.05 µCi [1-<sup>14</sup>C] palmitoyl-CoA. After 10 min incubation at 37°C, the reactions were stopped and lipids were extracted by the method of Bligh and Dyer (19) and separated by TLC on prefab silica G plates in a solvent system of petroleum ether/diethyl ether 80:20 (v/v) in an atmosphere of 10% ammonia. The TAG spot was scraped off, and the radioactivity was determined by liquid scintillation counting.

### Electron microscopy

After incubation for 24 h at 33 or 40°C, CHO-K1 and MT58 cells were fixed with Karnovsky fixative for 24 h, postfixed in 2% OsO<sub>4</sub> buffered in 0.1 M cacodylate buffer, dehydrated in a graded series of ethanol, and embedded in Durcupan AMC. Ultrathin sections were stained with 2.5% aqueous uranyl acetate and with 0.5% lead citrate. Specimens were examined and photographed using an EM Philips CM 10 EX electron microscope (Philips, Eindhoven) at 75 kV.

For immunoelectron microscopy, MT58 cells were fixed with 2% paraformaldehyde and 0.2% glutaraldehyde for 2 h. After scraping the cells from the dish and embedding them in 10% gelatin, small blocks were cut and incubated in 2.3 M sucrose at 4°C overnight and subsequently frozen in liquid nitrogen. Ultrathin sections (50–60 nm) were cut on a Leica Ultracut T equipped with a cryo-unit and picked up with sucrose/methylcellulose on Formvar carbon-coated copper grids. Sections were immunolabeled with α-PDI mAb (1:100), followed by RαM IgG (1:400) and protein A conjugated to 10 nm gold (1:80). Subsequently, the sections were contrasted with 0.2% uranyl oxalate (pH 7) and 0.4% uranyl acetate in 1.8% methylcellulose. Specimens were analyzed with a FEI Technai 12 electron microscope (Eindhoven) at 80 kV.

### Immunofluorescence microscopy and fluorescence recovery after photobleaching

CHO-K1 and MT58 cells were grown on glass coverslips. Incubations were started by shifting the cells to 40°C or leaving them at 33°C (control). After 24 h of incubation, cells were fixed with

4% paraformaldehyde in PBS and permeabilized with 0.1% saponin in PBS. After preincubation with PBS containing 2% BSA, cells were incubated with the primary antibody for 1 h at room temperature. Cells were washed three times for 5 min with PBS containing 1% BSA and then incubated with fluorophore-conjugated secondary antibodies for 1 h. For staining of the LDs, cells were fixed with 4% paraformaldehyde in PBS, followed by Bodipy 493/503 (final concentration 0.02  $\mu\text{g}/\text{ml}$ ) for 15 min at room temperature. Specimens were analyzed using a LEICA DMR fluorescence microscope or Leica TCS SP confocal laser scanning microscope. Images were analyzed using Image J software.

For studying the protein secretion and transport efficiency in MT58 cells, cells transiently transfected with plasmid containing the coding sequence for vesicular stomatitis virus glycoprotein fused to green fluorescent protein (pVSVG-GFP) were incubated at 40°C for 24 h and transferred to 33°C for 0, 12, or 60 min. Cells were fixed, stained, and analyzed as described above.

Fluorescence recovery after photobleaching (FRAP) studies were performed on MT58 ER-YFP cells cultured for 24 h at 40 or 33°C using a Bio-Rad 2100MP confocal microscope equipped with LaserSharp 2000 software for data acquisition. YFP was bleached within a defined region of interest with iterations of 50% 488 nm laser power, and subsequent recovery was monitored. Images were analyzed using Image J software.

### Gaussia luciferase transport assay

CHO-K1 and MT58 cells were transiently transfected with pC-MV-Gluc (New England Biolabs, Ipswich MA), containing the coding sequence for secreted Gaussia Luciferase, and after 2 h recovery shifted to 40°C or left at 33°C. After 24 h incubation, the medium was collected and cells were lysed by Luciferase Cell Lysis Buffer (New England Biolabs). Gluc activity in both fractions was measured by adding 20  $\mu\text{M}$  coelenterazine according to the manufacturer's protocol (Gaussia Luciferase Assay kit; New England BioLabs) and measured for 10 s in a luminometer. Gaussia luciferase secretion (relative light units (RLU) medium/RLU lysate) was expressed relative to the value of CHO-K1 secretion at 40°C (arbitrarily set to 1).

### Miscellaneous methods

Protein was determined by the method of Lowry as previously described (17). Statistical analyses were performed using a Student's *t*-test.

## RESULTS

### MT58 cells show an inhibited PC synthesis and an increased PC degradation

The CHO mutant cell line MT58 has a temperature-sensitive mutation in the CT $\alpha$  gene (18). In a previous study, we have shown that this mutation results in a decrease in PC synthesis by 80% in MT58 cells grown at the nonpermissive temperature of 40°C (17). Cellular membranes have a high turnover in PC, caused by a high rate of synthesis and breakdown (6). We therefore investigated which effect the inhibition of de novo synthesis of PC would have on the degradation of cellular PC in MT58 cells. MT58 cells and the wild-type CHO-K1 cells were prelabeled with [ $^3\text{H}$ ] choline for 48 h; thereafter, the breakdown of PC was measured. As shown in Fig. 1A, MT58 cells incubated at 33°C for 22 h still contained al-

most 80% of labeled PC compared with the 2 h time point and ~60% of label remained in CHO-K1 cells under the same conditions; the total PC mass in both cell lines is similar (17). In contrast, both wild-type and MT58 cells incubated at 40°C had only ~40% of the [ $^3\text{H}$ ]-labeled PC remaining after 22 h compared with the 2 h time point. The decreased amount of [ $^3\text{H}$ ] choline in PC at the permissive temperature was accompanied by 3- (MT58) to 5-fold (CHO-K1) higher levels of water-soluble choline products compared with cells incubated at 33°C (Fig. 1A). These results indicate that the breakdown of PC is accelerated in MT58 cells at the nonpermissive temperature and that it contributes to the rapid decline of the cellular PC content (13, 17) as it is not compensated for by an increase in synthesis of new PC, as in wild-type CHO cells.

### Inhibition of CT results in increased levels of intracellular neutral lipids in MT58 cells

To study the fate of the FA moieties of degraded PC in the MT58 cells at the nonpermissive temperature, we prelabeled the cells with trace amounts of [ $^3\text{H}$ ] oleate for 24 h, at which time point most of the intracellular label was in the phospholipid pool (mainly PC and phosphatidylethanolamine; cf. Fig. 1B), and chased the cells for 2 and 22 h in the absence of radiolabel. As shown in Fig. 1B, PC in MT58 cells at 33°C and in CHO-K1 cells at both temperatures retained >80% of their label. In MT58 cells chased for 20 h (from 2–22 h) at 40°C, the radiolabel in PC was lost for ~50%. The loss of [ $^3\text{H}$ ] oleate from PC in MT58 cells grown at 40°C was accompanied by a large increase of label in the TAG pool (Fig. 1B). The increase in [ $^3\text{H}$ ] oleate in the TAG pool correlated with the increase in total TAG in MT58 cells after incubation at 40°C (cf. Fig. 1B, C), suggesting that the FA moieties of the degraded PC are incorporated for a large part in TAG. The increase in TAG after a 24 h incubation period at the nonpermissive temperature (approximately 13 nmol/mg protein; Fig. 1C) also corresponds well with the loss of PC in that time period (30–40 nmol/mg protein, which would theoretically provide FAs for 20–27 nmol/mg protein of TAG; data not shown; cf. Ref. 17). The increased net formation of TAG did not depend on an induction of DGAT, the last enzyme in the synthesis of TAG, as the homogenates of MT58 cells cultured at 40°C did not show an increase in DGAT activity (Fig. 1C).

Most cells store their excess of TAG in cytosolic LDs, organelles consisting of a phospholipid monolayer and a core of neutral lipids (21). As shown in Fig. 2B, an increase in the amount of LDs is seen in MT58 cells cultured at the nonpermissive temperature in comparison to CHO-K1 cells grown at 40°C (Fig. 2A), in line with the increased level of TAG in these cells. In contrast, no significant differences in the number of LDs were observed in CHO-K1 and MT58 cells cultured at 33°C (Fig. 2F). To investigate whether PC-depleted MT58 displayed an increased LD fusion as seen in Cct knockdown *Drosophila* S2 cells (30), we incubated cells with 200  $\mu\text{M}$  oleic acid for 24 h. Incubation at the nonpermissive temperature resulted in an increase in the size of the numerous present LDs (Fig. 2E).



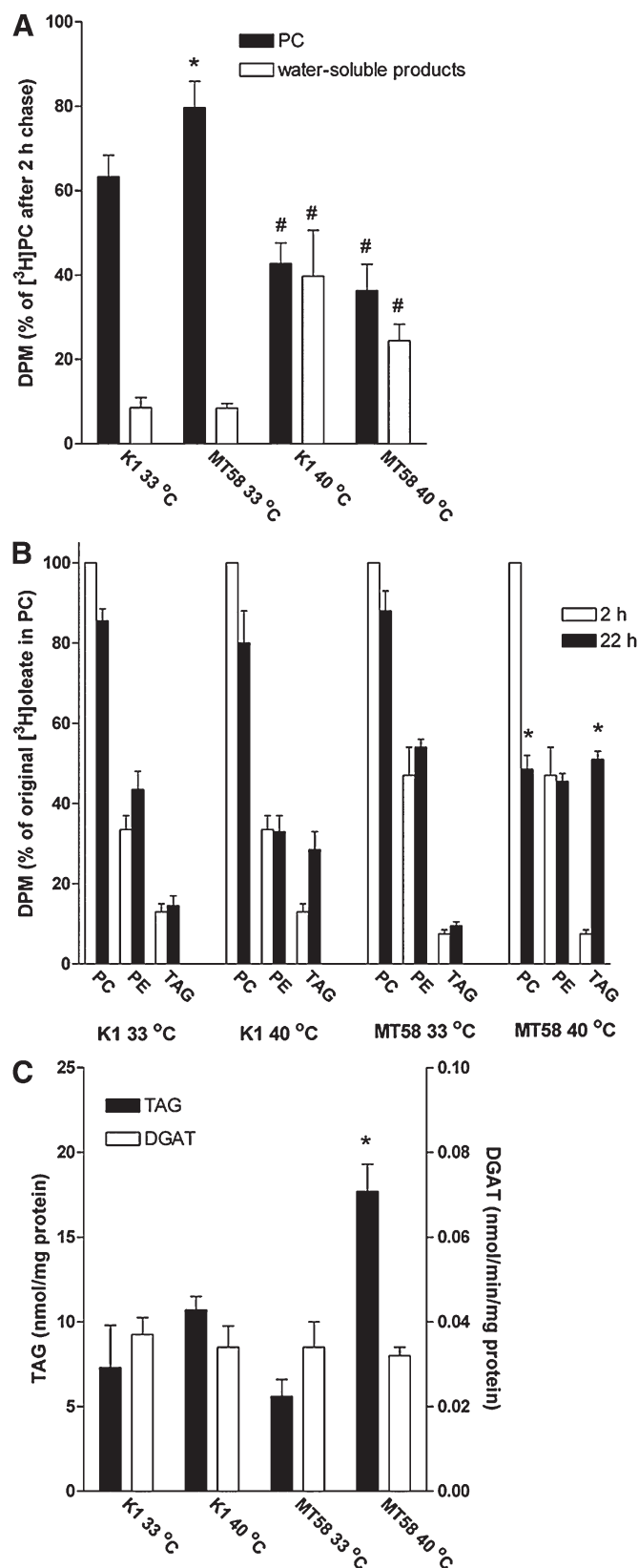


**Fig. 1.** A: Effect of the nonpermissive temperature on PC breakdown in MT58 cells. CHO-K1 and MT58 cells were grown at 33°C for 24 h and subsequently labeled with 2  $\mu$ Ci [<sup>3</sup>H] choline for 48 h. After labeling, the cells were incubated at 40°C for a period of 22 h in nonlabeled choline containing medium. Lipids and water-soluble compounds were extracted, and lipids were analyzed by TLC. The label present in PC (black bars) or water-soluble compounds

A similar enlargement of LDs was observed in oleic acid-treated CHO-K1 cells (Fig. 2D).

### PC depletion results in changes in ER structure and integrity

The inability of MT58 cells to synthesize PC at the nonpermissive temperature and the observed, increased breakdown of this major membrane component is likely to influence the overall structure of the cell, which was investigated by electron microscopy (EM) studies. As already seen in the neutral lipid staining at light microscopy level (Fig. 2B), numerous LDs were observed in the PC-depleted cells (Fig. 2C). The morphology of the mitochondria, nuclear, and plasma membrane (Fig. 3A, B) and the Golgi complex (Fig. 7) was not affected by the decrease in PC as observed by EM and immunofluorescence studies. However, we observed dilated tubular and spherical structures in 70–80% of the PC-depleted MT58 cells (Fig. 3A, B), enclosed by electron-dense ribosomes, which suggests a rough ER (rER) origin. Immunolabeling of these structures with an antibody against the ER protein PDI (Fig. 3C) revealed that the ER, normally a tubular membrane network enclosing a single luminal space, is largely dilated in these cells. PDI staining at the light microscopy level clearly demonstrated that the dilated, spherical ER structures were mainly localized at opposite sides of the nucleus (Fig. 3F). These ER spherules were induced by culturing at the nonpermissive temperature, as PDI localization in MT58 cells grown at 33°C (Fig. 3D) was similar to that in CHO-K1 cells incubated at 40°C (Fig. 3E) and 33°C (data not shown).

To investigate these ER spherules in detail, we stably transfected MT58 cells with a YFP construct containing the KDEL-ER retention signal. As shown in Fig. 4B, the ER-targeted YFP in MT58 cells at 40°C localize in spherical structures, similar to PDI localization at the nonpermissive temperature. Subsequent addition of lysoPC to the MT58 cells restored the normal ER morphology (Fig. 4C), demonstrating that the morphological change of the ER was reversible and not primarily caused by improper folding of CT itself.

(open bars) after 22 h incubation was expressed relative to the amount of label present in PC after 2 h. The results represent the means  $\pm$  SEM of three experiments, performed in triplicate. \* $P$  < 0.05, MT58 versus CHO-K1. # $P$  < 0.05, 40°C versus 33°C. B: Redistribution of the oleate moiety of PC in MT58 cells after inhibition of de novo PC synthesis. CHO-K1 and MT58 cells were grown at 33°C for 24 h and labeled with 1  $\mu$ Ci [<sup>3</sup>H] oleate for 24 h. After labeling, the cells were incubated at 33 or 40°C for a period of 2 (open bars) or 22 h (closed bars). Lipids were extracted and analyzed by TLC. The results represent the means  $\pm$  SEM of three experiments, performed in triplicate. \* $P$  < 0.05, MT58 versus CHO-K1. C: Increase in TAG in MT58 cells is not accompanied by increased DGAT activity. CHO-K1 and MT58 cells were cultured for 24 h at 33 or 40°C. DGAT activity (open bars) and intracellular TAG (closed bars) were determined after homogenization as described in Materials and Methods. The results represent the means  $\pm$  SEM of three experiments, performed in triplicate. \* $P$  < 0.05, MT58 versus CHO-K1.

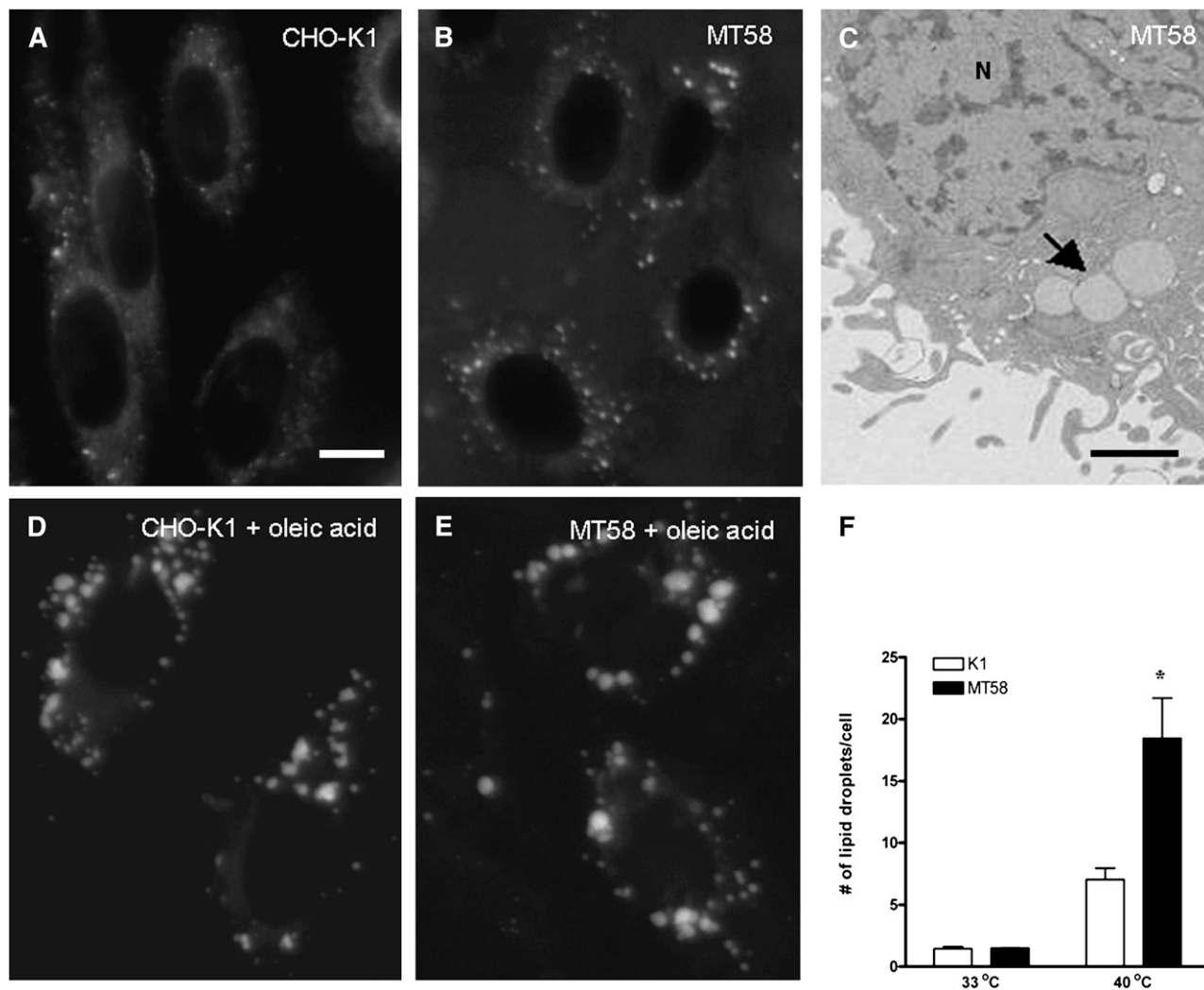


**Fig. 2.** Inhibition of PC synthesis results in an accumulation of LDs. Analysis of the neutral lipid content of CHO-K1 (A, D) and MT58 cells (B, C, E) cultured for 24 h at 40°C in the absence (A–C) or presence of 200  $\mu$ M oleic acid (D, E) by fluorescence microscopy after Bodipy staining and transmission electron microscopy (C). Arrow indicates LDs. N, nucleus. Total number of LDs in CHO-K1 and MT58 cells at 33 and 40°C in the absence of oleic acid was quantified using Image J software (F). The results represent the means  $\pm$  SEM performed in 100 cells. \* $P < 0.05$ , MT58 versus CHO-K1. Bar = 10  $\mu$ m in A and 500 nm in C.

When the formation of the ER sphericles was followed in time in MT58 ER-YFP cells, it was observed that small punctuated ER structures appeared 6 h after inhibition of PC synthesis, which seemed to fuse to larger ER sphericles (data not shown). As the ER and the microtubule network are highly interdependent structures, we tested whether microtubule-driven motors were involved in the formation of the large dilated ER sphericles. After treatment of MT58 ER-YFP cells with nocodazole, an inhibitor of microtubule formation, no large ER sphericles were observed. Instead, smaller dispersed ER structures appeared throughout the cytoplasm (Fig. 4E).

Since the ER sphericles seemed to coexist with tubular ER in MT58 cells (Fig. 4B, F), we investigated whether the spherical structures were still in connection with this normal pool of ER or if dilated regions formed individual structures. For this purpose, we performed FRAP on the affected ER parts in MT58 ER-YFP cells. The ER sphericles were photobleached, and images were collected to moni-

tor the diffusion of ER-YFP into the photobleached region. Considering the loss of fluorescence signal of the bleached region (Fig. 5B), full recovery was observed (Fig. 5C), indicating a close connection of the sphericles and the remaining part of the ER.

#### PC inhibition is accompanied by impairment in the protein transport from Golgi complex toward plasma membrane in MT58 cells

The observation that the sphericles and normal ER parts were still connected suggests that the ER might be largely functionally intact and, therefore, that secretion and transport of proteins still occurs in MT58 cells. To study the exocytic membrane transport, we transiently transfected CHO-K1 and MT58 cells with pVSVG-GFP, a temperature-sensitive vesicular stomatitis virus glycoprotein fused to GFP. VSVG misfolds and accumulates in the ER at 40°C (which coincides with the nonpermissive temperature of MT58 cells) and is rapidly folded and transported synchro-

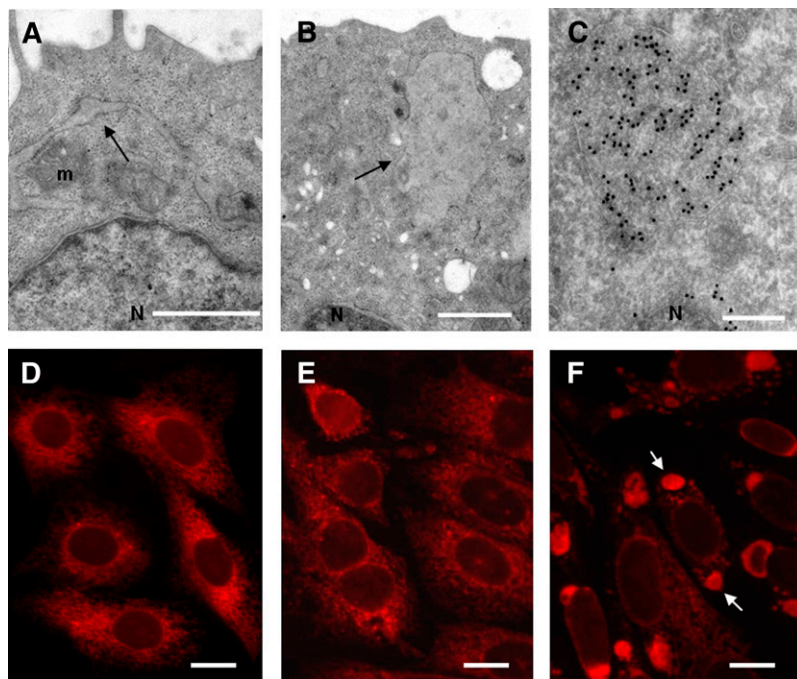


**Fig. 3.** Dilatation of the rER in PC-depleted MT58 cells. Thin section electron micrographs of MT58 cells cultured at 40°C for 24 h, showing dilated, tubular ER (A) and ER sphericles (B). Immunolabeling of MT58 cells with anti-PDI antibody and 10 nm gold-coupled secondary antibody, showing luminal staining of the ER sphericles (C). For fluorescence microscopy analysis, CHO-K1 (E) and MT58 cells (D, F) were cultured at 32°C (D) or 40°C (E, F) for 24 h and stained with an antibody against ER marker PDI. Arrow indicates ER sphericles localized on both sides of the nucleus (N). m, mitochondria. Bar = 500nm in A and B, 200 nm in C, and 10  $\mu$ m in D–F.

nously via the Golgi complex to the plasma membrane upon a temperature shift to 33°C (22).

In MT58 cells, it was seen that in contrast to the ER-resident protein PDI, VSVG-GFP did not accumulate in the dilated ER regions and that in comparison with the wild-type CHO-K1 cells, the protein synthesis was not affected in these cells (Fig. 6). However, we found a significant difference in the transport of the VSVG protein in MT58 cells toward the plasma membrane. After 1 h of incubation at 33°C, a large percentage of VSVG proteins was transported to the plasma membrane in CHO-K1 cells. In contrast, in MT58 cells, only a small amount of VSVG was found at the plasma membrane (Fig. 6A). A prolonged incubation of 2 h at 33°C did not result in an increased VSVG staining of the plasma membrane (data not shown). Furthermore, staining of nonpermeabilized cells with a monoclonal antibody directed against the extracellular domain of VSVG showed a lower VSVG labeling on the plasma membrane in MT58 cells compared with CHO-K1 cells (Fig. 6B, upper panels), pointing out that protein transport along the secretory pathway is defective in PC-depleted MT58 cells. Protein transport in CHO-K1 and MT58 was also studied by transfecting cells with a vector encoding secreted Gaussia luciferase. Consistent with the VSVG data, we observed an intracellular accumulation of Gaussia luciferase, and therefore a lower relative secretion, in PC-depleted MT58 cells (Fig. 6C). Addition of lysoPC to MT58 cells restored both VSVG transport to the plasma membrane (Fig. 6B, lower panels) as well as secretion of Gaussia luciferase into the medium (Fig. 6C).

In order to investigate at which subcellular level this PC-induced impairment occurs, we shifted MT58 and wild-type cells after VSVG-GFP transfection to 20°C, to block transport of proteins from the Golgi complex to the plasma membrane (23). In both MT58 and wild-type cells, we found VSVG accumulation in the Golgi complex (Fig. 7),

indicating a normal ER-Golgi transport. However, after shifting the cells again to 33°C to permit transport to the plasma membrane, we observed in MT58 cells a sustained accumulation of VSVG in the Golgi complex, whereas in the wild-type cells, most GFP-labeled proteins were found on the plasma membrane. These results indicate that the inhibition of PC synthesis specifically impairs the protein transport from the Golgi complex toward the plasma membrane.

## DISCUSSION

MT58 cells incubated for 24 h at the nonpermissive temperature have a drastic decreased cellular PC content but are still viable with a growth rate comparable to CHO-K1 and can be rescued from apoptosis by addition of lysoPC around 30 h (13, 17). Therefore, we used this model to investigate the effects of inhibition of PC synthesis on PC breakdown and morphological and functional changes in these cells.

MT58 cells have a lower CT activity at 33°C compared with the wild-type CHO-K1 cell line but can nevertheless maintain their PC levels (17). In this study, we show that MT58 cells grown at 33°C retain a higher percentage of labeled choline in their PC pool compared with CHO-K1 cells. Although we cannot formally exclude the possibility that MT58 cells have a higher reincorporation of labeled choline in PC, we consider that it is more likely that this reflects a lower degradation of PC for several reasons. First, a relatively high excess of unlabeled choline was added during the chase to prevent reincorporation of released label. Second, MT58 cells have a lower rate of PC synthesis than the wild-type cell line at 33°C. A lower degradation of PC in MT58 cells at 33°C would compensate for the reduced PC synthesis. However, such a “brake” on



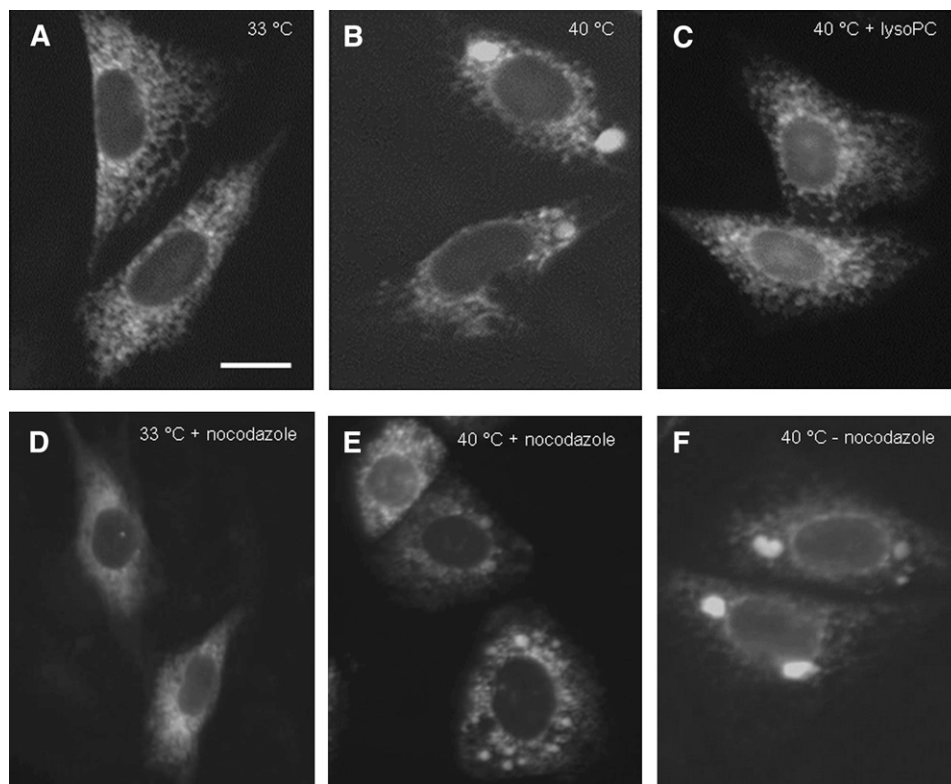


**Fig. 4.** Dilution of the rER in PC-depleted MT58 cells is influenced by microtubule activity and can be restored by addition of lysoPC. To study the reversibility of the formed ER sphericles, MT58 cells stably expressing ER-YFP were cultured at 33°C (A) or 40°C (B) for 24 h. To cells cultured at 40°C for 24 h, 50  $\mu$ M lysoPC was added for another 24 h at 40°C (C). To examine microtubule involvement in the formation of ER sphericles, MT58 ER-YFP cells were treated with 10  $\mu$ M nocodazole for 24 h at 33°C (D), 40°C (E), or cultured at 40°C without nocodazole treatment (F). Bar = 10  $\mu$ m.

PC degradation is apparently lost when culturing MT58 cells at the nonpermissive temperature. This may suggest a difference in the regulation of the enzyme responsible for breakdown of PC at 33 and 40°C. Alternatively, degradation of PC at the permissive and restricted temperature may be performed by different enzymes. In fact, multiple enzymes have been implicated in the degradation of PC at various conditions, including a calcium-independent phospholipase A<sub>2</sub>, which was active during enhanced PC turnover (24, 25), and the neuropathy target esterase responsible in yeast and mammalian cells for formation of glycerophosphocholine (26).

Another consequence of the inactivation of CT is that the degradation products of PC, including free FAs, DAG, phosphocholine, and glycerophosphocholine, cannot be recycled in the CDP-choline pathway anymore. As high concentrations of FFAs are toxic to the cell (27), FAs are incorporated in neutral lipids, like TAG. As observed by electron and fluorescence microscopy, incubation of MT58 cells at 40°C leads to the formation of LDs. These LDs presumably form as a consequence of the rise in TAG levels observed here and also described previously (28, 29). We show that the FAs converted into TAG are mainly derived from the degraded PC (Fig. 1B), providing further evidence for the relation between phospholipid metabolism and TAG/LD formation. This link is further strength-

ened by Guo et al. (30), who also observed an increased TAG content in *Cct1* knockdown *Drosophila* S2 cells. However, in oleic acid-treated cells, they found only few very large LDs as a result of enhanced LD fusion. In contrast, oleic acid-treated MT58 cells have numerous large LDs (Fig. 2E), similar to the oleic acid-induced LDs in CHO-K1 cells. Even treatment with relative high oleic acid concentrations (1 mM) did not increase LD fusion in the MT58 cells (data not shown).

Interestingly, Caviglia et al. (31) observed that MT58 has lower levels of TAG than CHO-K1 cells at the permissive temperature. This was supposedly caused by a relatively fast degradation of TAG, not compensated for by a somewhat higher rate of TAG synthesis, due to an increase in acyl-coA synthase, mitochondrial glycerol-3-phosphate acyltransferase, and DGAT activity (31). We also found somewhat lower amounts of TAG and LDs in MT58 cells compared with K1 cells at 33°C (Figs. 1B and 2F), although we could not observe a difference in DGAT activity between the cell lines (Fig. 1C). A possible increased degradation of TAG in MT58 at the nonpermissive temperature, similar as described by Caviglia, in combination with the observed increase in PC degradation, would result in elevated levels of lipotoxic FAs or derivatives thereof, which may contribute to the final apoptotic response in the MT58 cells.

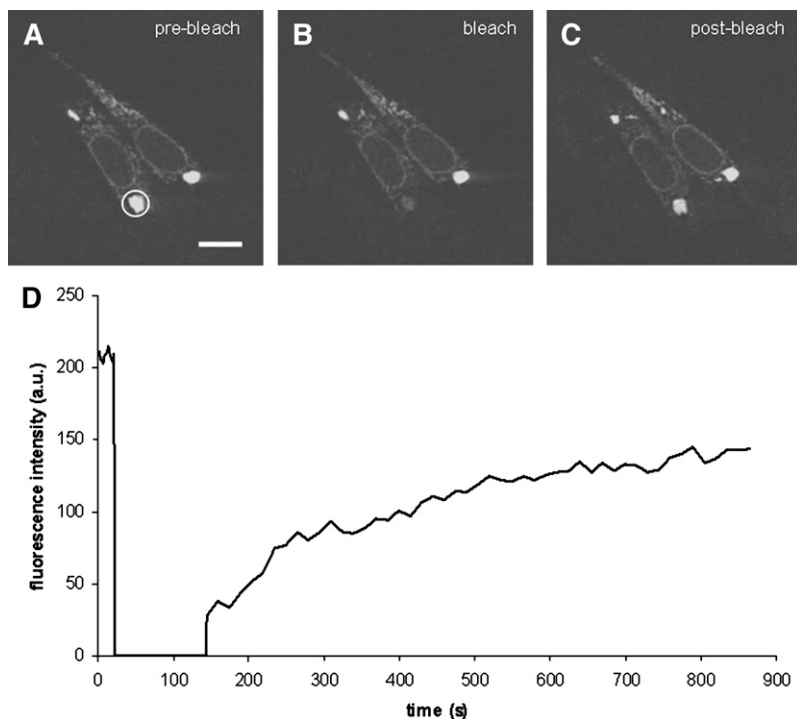


**Fig. 5.** FRAP analysis to determine the connectivity of ER sphericles to unaffected ER in MT58 cells. MT58 cells stably expressing ER-YFP were cultured at 40°C for 24 h. ER sphericles were bleached by iterations of 50% 488 nm laser power. Images were captured before (A; prebleach, white circle indicates the region to be bleached), immediately after (B; bleach), and after photobleaching (C; postbleach). Fluorescence was measured in the bleached regions of interest and plotted against time (D). Bar = 10  $\mu$ m.

The loss of approximately half of its major membrane-building component is expected to influence the structure of membranes in MT58 cells grown at 40°C. After 24 h of PC depletion, the structure of the plasma membrane, nuclear membrane, Golgi complex, and mitochondria seems to be morphologically intact. In contrast, a part of the ER apparently lost its reticular structure as dilated and spherical ER structures are observed. As ER membranes constitute on average ~50% of the total cellular membranes (32), it might be expected that a reduction of 50% in PC level will affect the PC content of the ER structure profoundly and, therefore, its function. The transition of a reticular to the observed spherical structure may reflect a way to preserve the integrity of an organelle when faced with a shortage of the major membrane component, due to the more efficient volume-to-surface ratio of a spherical structure. It is conceivable that the ER also serves as a “PC reservoir” to maintain the PC level and, thus, function of less adaptive membrane structures like mitochondria and the plasma membrane. Typically, in PC-depleted MT58 cells, only the rER is partially affected. Other subpools of the ER, like the smooth (s)ER, which can be morphologically distinguished from rER on the EM level, and transitional (t) ER, defined by sec23 Ab staining, seemed to be morphologically intact, stressing the existence of specialized ER regions with different behavior to changes in lipid profile.

The cause of ER sphericle formation in MT58 cells is unknown. It has been described that the ER tubular structure is sensitive to ER stress, like  $\text{Ca}^{2+}$  overload (33) and addition of palmitic acid, a lipotoxic compound (34). When cells are faced with one of these stresses, a process known as the ER stress response is induced (35). ER stress might also result in the formation of ER-containing autophagosomal structures (36). However, in previous stud-

ies we did not observe an ER stress response in MT58 cells grown at the nonpermissive temperature (17, 37). We could not prove the presence of autophagosome markers in PC-depleted cells (data not shown), thereby excluding the possibility of ER stress-induced ER-containing autophagosomes (36).

As the ER is morphologically heavily affected in MT58 cells, the main ER functions, protein synthesis, folding, and transport, might be impaired. We previously found that the protein synthesis is not inhibited in MT58 cells at 40°C (17). The VSVG experiments demonstrate that the expression of VSVG and its transport from the ER toward the Golgi complex is likewise not affected. However, despite the fact that the Golgi complex seems morphologically intact, we observe an inhibited protein transport from the Golgi complex toward the plasma membrane in PC-depleted MT58 cells, which could be rescued by addition of exogenous PC. The importance of a balanced PC synthesis on protein transport is further underlined by recent experiments performed in CCT $\alpha$ -deficient macrophages, in which cytokine secretion was shown to be impaired (38). Whereas the group of Jackowski only found an inhibited effect on regulated secretion induced by lipopolysaccharide, we also showed an impairment of constitutive secretion. It might have to be taken into account that we use an inducible CCT $\alpha$ -deficient cell line in our experiments, in comparison to a permanent CCT $\alpha$  knockout cell line in where adaptation can occur. Besides, the distribution of trans-Golgi network (TGN) markers in lipopolysaccharide-treated CCT $\alpha^{-/-}$  macrophages does not resemble our Golgi morphology after blocking the constitutive secretion, which might suggest that in macrophages a permanent CCT $\alpha$  knockout directly affects TGN morphology.



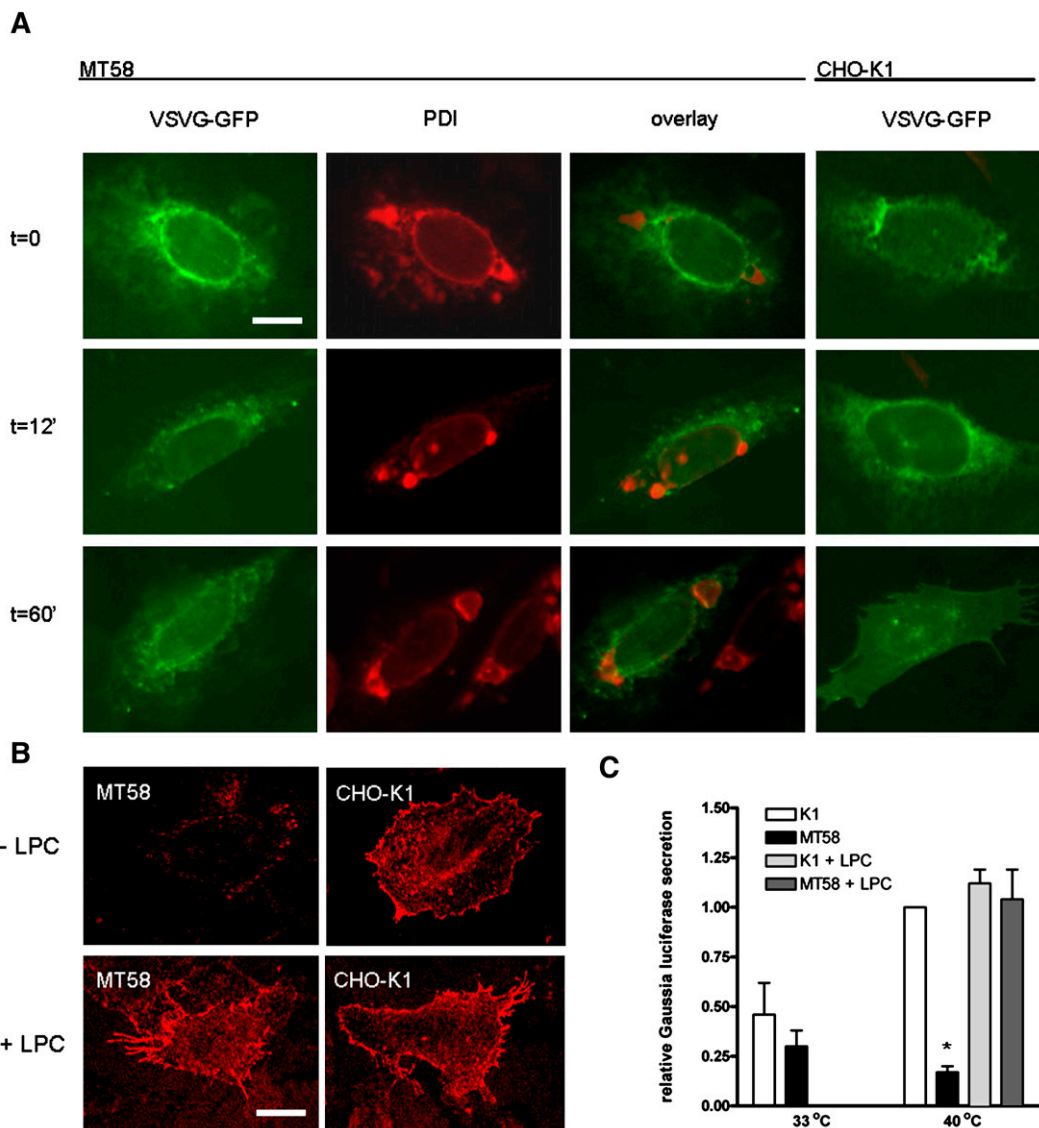


**Fig. 6.** A: VSVG transport to the plasma membrane is impaired in PC-depleted MT58 cells. MT58 and CHO-K1 transiently transfected with VSVG-GFP were cultured for 24 h at 40°C and shifted to 33°C. Cells were subsequently fixed at the indicated time. After fixation, cells were stained with PDI antibody. VSVG-GFP (direct fluorescence) is green, and PDI is red. Bar = 10  $\mu$ m. B: Impaired VSVG transport in PC-depleted MT58 cells can be restored by lysoPC addition. Transiently VSVG-GFP transfected MT-58 cells and CHO-K1 cells were cultured in the absence or presence of 50  $\mu$ M lysoPC during the 40°C incubation period (24 h). Cells were subsequently shifted to 33°C for 1 h and fixed and stained under nonpermeabilizing conditions with an antibody directed against the extracellular domain of VSVG (red). Bar = 10  $\mu$ m. C: Gaussia luciferase secretion is impaired in PC-depleted MT58 cells. Gaussia luciferase was measured in medium and cell lysate of transiently transfected MT58 and CHO-K1 cells incubated at 33 or 40°C. For experimental details, see Materials and Methods. Gaussia luciferase secretion (RLU medium/RLU lysate) is expressed relative to the value of CHO-K1 secretion at 40°C (arbitrarily set to 1). To investigate whether the impaired secretion was dependent on PC, 50  $\mu$ M lysoPC was added during the 40°C incubation period. The results represent the means  $\pm$  SEM of three experiments performed in triplicate. \* $P < 0.05$ , MT58 versus CHO-K1.


The necessity of lipids in Golgi-mediated transport is increasingly discussed. DAG and phosphatidic acid are both needed for the vesicular transport of proteins from the TGN, possibly by induction of membrane bending and formation of highly curved membranes (39, 40). It is also found that DAG can recruit and activate proteins required for protein transport, like the vesicle biogenesis factor protein kinase D (PKD). Binding of PKD to DAG is essential for its recruitment to the TGN where it can form specific

transport vesicles (41). Reduction of DAG levels results in an inhibited PKD recruitment and blocked protein transport to the cell surface (41), thus stressing the importance of maintaining certain DAG concentrations. The precise mechanisms to maintain DAG levels in the Golgi complex are not yet known. Nevertheless, there are indications that the PC metabolism might be involved in DAG regulation by interactions of PI-transfer proteins sec-14 (yeast) and Nir 2 (mammalian) (42, 43).

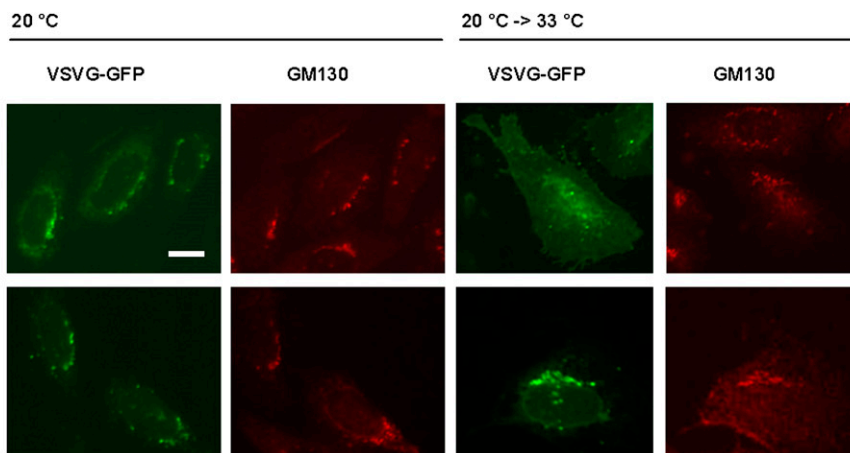


**Fig. 7.** VSVG protein accumulates in the Golgi complex in PC-depleted MT58 cells. MT58 and CHO-K1 cells transiently transfected with VSVG-GFP were cultured for 24 h at 40°C and shifted to 20°C for 1 h to block protein transport from the Golgi complex toward the plasma membrane. Thereafter, cells were fixed or incubated for another hour at 33°C. After fixation cells were stained with an antibody against *cis*-Golgi marker GM130. VSVG-GFP (direct fluorescence) is green, and GM130 is red. Bar = 10  $\mu$ m.

In MT58 cells, the intracellular DAG balance might be disturbed by the inhibition of PC synthesis. On one hand, it can be expected that DAG levels will rise, as DAG is not longer used in the formation of PC (43). However, on the other hand, the decrease in intracellular PC level is expected to lead to a decrease in the generation of DAG from PC (e.g., by sphingomyelin synthase and by phospholipases C and D). Furthermore, since DAG may also be converted in TAG by the release of FAs during the degeneration of PC, the overall effect of inhibiting PC synthesis in the MT58 cells on DAG levels in a particular membrane compartment is hard to predict. In earlier experiments, we already showed that total cellular DAG levels are decreased in PC-depleted MT58 cells (44). It might be interesting to know if the DAG concentration is specifically altered in the Golgi complex of PC-depleted MT58 cells as well.

Our PC-depleted MT58 cell model might be a nice system to get more insight in the relation of ER and Golgi complex and the mechanisms in which lipids are involved in the secretory pathway. Ongoing studies on lipid profiles of the Golgi complex and the exact localization of protein transport impairment in PC-depleted cells should give more insight in these processes. 

The authors thank M. Molenaar and M. Hassan Zade Nadjari for technical assistance and the Center for Cell Imaging, Faculty of Veterinary Medicine, Utrecht University and the EM facility of the Faculty of Biology, Utrecht University, for using their equipment and expertise. We thank Prof. Dr. Pepperkok for the antibody against the extracellular domain of VSVG.

## REFERENCES

- Kent, C. 1990. Regulation of phosphatidylcholine biosynthesis. *Prog. Lipid Res.* **29**: 87–105.
- Exton, J. H. 1994. Phosphatidylcholine breakdown and signal transduction. *Biochim. Biophys. Acta.* **1212**: 26–42.
- Billah, M. M., and J. C. Anthes. 1990. The regulation and cellular functions of phosphatidylcholine hydrolysis. *Biochem. J.* **269**: 281–291.
- Kiss, Z. 1990. Effects of phorbol ester on phospholipid metabolism. *Prog. Lipid Res.* **29**: 141–166.
- Nishizuka, Y. 1995. Protein kinase C and lipid signaling for sustained cellular responses. *FASEB J.* **29**: 484–496.
- Jackowski, S. 1996. Cell cycle regulation of membrane phospholipid metabolism. *J. Biol. Chem.* **271**: 20219–20222.
- Houweling, M., Z. Cui, C. D. Abfuso, M. Bussiere, M. H. Chen, and D. E. Vance. 1996. CTP-phosphocholine cytidyltransferase is both a nuclear and cytoplasmic protein in primary hepatocytes. *Eur. J. Cell Biol.* **69**: 55–63.
- Lykidis, A., I. Baburina, and S. Jackowski. 1999. Distribution of CTP:phosphocholine cytidyltransferase (CCT) isoforms. Identification of a new CCTbeta splice variant. *J. Biol. Chem.* **274**: 26992–27001.
- Kent, C. 1997. CTP:phosphocholine cytidyltransferase. *Biochim. Biophys. Acta* **1348**: 79–90.
- Dunne, S. J., R. B. Cornell, J. E. Johnson, N. R. Glover, and A. S. Tracey. 1996. Structure of the membrane binding domain of CTP:phosphocholine cytidyltransferase. *Biochemistry.* **35**: 11975–11984.
- Cornell, R. B. 1998. How cytidyltransferase uses an amphipathic helix to sense membrane phospholipid composition. *Biochem. Soc. Trans.* **26**: 539–544.
- Baburina, I., and S. Jackowski. 1998. Apoptosis triggered by 1-O-octadecyl-2-O-methyl-rac-glycero-3-phosphocholine is prevented by increased expression of CTP:phosphocholine cytidyltransferase. *J. Biol. Chem.* **273**: 2169–2173.
- Esko, J. D., M. Nishijima, and C. R. Raetz. 1982. Animal cells dependent on exogenous phosphatidylcholine for membrane biogenesis. *Proc. Natl. Acad. Sci. USA.* **79**: 1698–1702.
- Esko, J. D., M. M. Wermuth, and C. R. Raetz. 1981. Thermolabile CDP-choline synthetase in an animal cell mutant defective in lecithin formation. *J. Biol. Chem.* **256**: 7388–7393.
- Esko, J. D., and C. R. Raetz. 1980. Autoradiographic detection of animal cell membrane mutants altered in phosphatidylcholine synthesis. *Proc. Natl. Acad. Sci. USA.* **77**: 5192–5196.
- Cui, Z., M. Houweling, M. H. Chen, M. Record, H. Chap, D. E. Vance, and F. Terce. 1996. A genetic defect in phosphatidylcholine biosynthesis triggers apoptosis in Chinese hamster ovary cells. *J. Biol. Chem.* **271**: 14668–14671.
- van der Sanden, M. H. M., M. Houweling, L. M. G. van Golde, and A. B. Vaandrager. 2003. Inhibition of phosphatidylcholine synthesis induces expression of the endoplasmic reticulum stress and apoptosis related protein C/EBP-Homologous Protein (CHOP/GADD153). *Biochem. J.* **369**: 643–650.
- Sweitzer, T. D., and C. Kent. 1994. Expression of wild-type and mutant rat liver CTP: phosphocholine cytidyltransferase in a

- cytidyltransferase-deficient Chinese hamster ovary cell line. *Arch. Biochem. Biophys.* **311**: 107–116.
19. Bligh, E. G., and W. J. Dyer. 1959. A rapid method of total lipid extraction and purification. *Can. J. Biochem. Physiol.* **37**: 911–917.
  20. Wieland, O. H. 1984. Glycerol UV-method. In *Methods of Enzymatic Analysis*. Vol. 6. H. U. Bergmeyer, editor. Verlag Chemie, Weinheim, Germany. 504–510.
  21. Martin, S., and R. G. Parton. 2006. Lipid droplets: a unified view of a dynamic organelle. *Nat Rev Mol Cell Biol* **7**: 373–378.
  22. Hirschberg, K., C. M. Miller, J. Ellenberg, J. F. Presley, E. D. Siggia, R. D. Phair, and J. Lippincott-Schwartz. 1998. Kinetic analysis of secretory protein traffic and characterization of Golgi to plasma membrane transport intermediates in living cells. *J. Cell Biol.* **143**: 1485–1503.
  23. Griffiths, G., S. Pfeiffer, K. Simons, and K. Matlin. 1985. Exit of newly synthesized membrane proteins from the trans cisterna of the Golgi complex to the plasma membrane. *J. Cell Biol.* **101**: 949–964.
  24. Baburina, I., and S. Jackowski. 1999. Cellular responses to excess phospholipids. *J. Biol. Chem.* **274**: 9400–9408.
  25. Barbour, S. E., A. Kapur, and C. L. Deal. 1999. Regulation of phosphatidylcholine homeostasis by calcium-independent phospholipase A2. *Biochim. Biophys. Acta.* **1439**: 77–88.
  26. Zaccheo, O., D. Dinsdale, P. A. Meacock, and P. Glynn. 2004. Neuropathy target esterase and its yeast homologue degrade phosphatidylcholine to glycerophosphocholine in living cells. *J. Biol. Chem.* **279**: 24024–24033.
  27. Martins de Lima, T., M. F. Cury-Boaventura, G. Giannocco, M. T. Nunes, and R. Curi. 2006. Comparative toxicity of fatty acids on a macrophage cell line (J774). *Clin. Sci.* **111**: 307–317.
  28. Jackowski, S., J. Wang, and I. Baburina. 2000. Activity of the phosphatidylcholine biosynthetic pathway modulates the distribution of fatty acids into glycerolipids in proliferating cells. *Biochim. Biophys. Acta.* **1483**: 301–315.
  29. Waite, K. A., and D. E. Vance. 2000. Why expression of phosphatidylethanolamine N-methyltransferase does not rescue Chinese hamster ovary cells that have an impaired CDP-choline pathway. *J. Biol. Chem.* **275**: 21197–21202.
  30. Guo, Y., T. C. Walther, M. Rao, N. Stuurman, G. Goshima, K. Terayama, J. S. Wong, R. D. Vale, P. Walter, and R. V. Farese, Jr. 2008. Functional genomic screen reveals genes involved in lipid droplet formation and utilisation. *Nature.* **453**: 657–661.
  31. Caviglia, J. M., I. N. De Gomez Dumm, R. A. Coleman, and R. A. Igal. 2004. Phosphatidylcholine deficiency upregulates enzymes of triacylglycerol metabolism in CHO cells. *J. Lipid Res.* **45**: 1500–1509.
  32. Bolender, R. P. 1974. Stereological analysis of the guinea pig pancreas. *J. Cell Biol.* **61**: 269–287.
  33. Dayel, M. J., E. F. Y. Hom, and A. S. Verkman. 1999. Diffusion of green fluorescent protein in the aqueous-phase lumen of endoplasmic reticulum. *Biophys. J.* **76**: 2843–2851.
  34. Borradaile, N. M., X. Han, J. D. Harp, S. E. Gale, D. S. Ory, and J. E. Schaffer. 2006. Disruption of endoplasmic reticulum structure and integrity in lipotoxic cell death. *J. Lipid Res.* **47**: 2726–2737.
  35. Rutkowski, D. T., and R. J. Kaufman. 2004. A trip to the ER: coping with stress. *Trends Cell Biol.* **14**: 20–28.
  36. Bernales, S., S. Schuck, and P. Walter. 2007. ER-phagy: selective autophagy of the endoplasmic reticulum. *Autophagy* **3**: 285–287.
  37. van der Sanden, M. H. M., H. Meems, M. Houweling, J. B. Helms, and A. B. Vaandrager. 2004. Induction of CCAAT/enhancer-binding protein (C/EBP)-homologous protein/growth arrest and DNA damage-inducible protein 153 expression during inhibition of phosphatidylcholine synthesis is mediated via activation of a C/EBP-activating transcription factor-responsive element. *J. Biol. Chem.* **279**: 52007–52015.
  38. Tian, Y., C. Pate, A. Andreolotti, L. Wang, E. Tuomanen, K. Boyd, E. Claro, and S. Jackowski. 2008. Cytokine secretion requires phosphatidylcholine synthesis. *J. Cell Biol.* **181**: 945–957.
  39. Mousley, C. J., K. R. Tyeryar, P. Vincent-Pope, and V. A. Bankaitis. 2007. The Sec14-superfamily and the regulatory interface between phospholipid metabolism and membrane trafficking. *Biochem. Biophys. Acta.* **1771**: 727–736.
  40. Corda, D., C. Hidalgo Carcedo, M. Bonazzi, A. Luini, and S. Spano. 2002. Molecular aspects of membrane fission in the secretory pathway. *Cell Mol. Life Sci.* **59**: 1819–1832.
  41. Baron, C. L., and V. Malhotra. 2002. Role of diacylglycerol in PKD recruitment to the TGN and protein transport to the plasma membrane. *Science.* **295**: 325–338.
  42. McGee, T. P., H. B. Skinner, E. A. Whitters, S. A. Henry, and V. A. Bankaitis. 1994. A phosphatidylinositol transfer protein controls the phosphatidylcholine content of yeast Golgi membranes. *J. Cell Biol.* **124**: 273–287.
  43. Litvak, V., N. Dahan, S. Ramachandran, H. Sabanay, and S. Lev. 2005. Maintenance of the diacylglycerol level in the Golgi apparatus by the Nir2 protein is critical for Golgi secretory function. *Nat. Cell Biol.* **7**: 225–234.
  44. van der Sanden, M. H. M., M. Houweling, D. Dijssings, A. B. Vaandrager, and L. M. G. van Golde. 2004. Inhibition of phosphatidylcholine is not the primary pathway in hexadecylphosphocholine-induced apoptosis. *Biochim. Biophys. Acta.* **1636**: 99–107.